J. Phys. Chem. A **2002,** *106,* 4998−5004

Infrared Matrix Isolation and Density Functional Theory Study of Intermediates in the Reactions of $OVCl_3$ and $CrCl_2O_2$ with H_2O

Bethany L. Subel, David A. Kayser, and Bruce S. Ault*

Department of Chemistry, University of Cincinnati, P.O. Box 210172, Cincinnati, Ohio 45221-0172

Received: January 16, 2002; In Final Form: March 21, 2002

Initial and secondary intermediates in the reactions of $OVCl_3$ and $CrCl_2O_2$ with H_2O have been characterized by matrix isolation infrared spectroscopy and density functional calculations. Twin jet co-deposition of these reagents led to a series of infrared absorptions that are assigned to the 1:1 molecular complexes between these two species. Irradiation of these matrices with light of $\lambda > 300$ nm led to complete destruction of the bands of complexes, and the growth of a number of new bands. These are assigned to the $Cl_2V(O)OH$ and $ClCr(O)_2OH$ species, as well as to HCl arising from destruction of the complex. Identification of these species was supported by isotopic labeling (^{18}O and ^{2}H), as well as by B3LYP/6-311G+(d,2p) and B3LYP/LANL2DZ density functional calculations. Good agreement was observed between the experimental and computed frequencies. The overall yield of product was low for these system, and was probably a consequence of the low basicity of H_2O.

Introduction

High-valent transition metal oxo compounds, including $OVCl_3$ and $CrCl_2O_2$, are very strong oxidizing agents and are known to oxidize a wide range of organic substrates. This oxidizing power has applications in catalysis as well as in organic synthesis.[1,2] However, very little is known about the reaction of these reagents with H_2O, despite its ubiquitous presence in nature. A single drop of either reagent will fume vigorously in the atmosphere, generating HCl and additional products. While the mechanistic details of this reaction have not yet been explored, one group[3] has employed this reactivity to produce thin films of V_2O_5 through the chemical vapor deposition reaction of $OVCl_3$ with H_2O.

The matrix isolation technique[4−6] was developed to facilitate the isolation and spectroscopic characterization of reactive intermediates. This approach has been applied to the study of a wide range of species, including radicals, weakly bound molecular complexes, and molecular ions. Recent studies from this laboratory have focused on the sequence of intermediates formed in the reactions of $OVCl_3$ and $CrCl_2O_2$ with small organic substrates,[7−10] as well as with NH_3.[11,12] These studies have demonstrated that these reactions occur through the formation of an initial 1:1 complex, followed by thermal and/or photochemical elimination of HCl. In addition, since impurity levels of water are always present in matrix isolation studies, a knowledge of the spectrum of possible reaction products of $OVCl_3$ and $CrCl_2O_2$ with H_2O is important. Consequently, a study was undertaken to identify and characterize initial and secondary intermediates in the reaction of $OVCl_3$ and $CrCl_2O_2$ with H_2O. Density functional calculations were also carried out in support of the experimental observations.

Experimental Details

All of the experiments in this study were carried out on conventional matrix isolation apparatus that has been described.[13] Chromyl chloride, $CrCl_2O_2$ and $OVCl_3$ (both Aldrich), were introduced into the vacuum system as the vapor above the room-temperature liquid, after purification by freeze−pump−thaw cycles at 77 K. H_2O (distilled), $H_2{}^{18}O$ (99% ^{18}O), and D_2O (99% D) (both Cambridge Isotope Laboratory) were introduced in a similar manner into a separate vacuum manifold and were purified by repeated freeze−pump−thaw cycles at 77 K. Argon and nitrogen (Wright Brothers) were used as the matrix gas in different experiments, and were used without further purification.

Matrix samples were deposited in both the twin jet and merged jet modes. In the former, the two gas samples were deposited from separate nozzles onto the 14 K cold window, allowing for only a very brief mixing time prior to matrix deposition. Several of these matrices were subsequently warmed to 33−35 K to permit limited diffusion and then recooled to 14 K and additional spectra recorded. In addition, most of these matrices were irradiated for 1.0 or more hours with the H_2O/Pyrex filtered output of a 200 W medium-pressure Hg arc lamp, after which additional spectra were recorded.

A few experiments were conducted in the merged jet mode,[14] in which the two deposition lines were joined with an UltraTorr tee at a distance from the cryogenic surface, and the flowing gas samples were permitted to mix and react during passage through the merged region. The length of this region was variable; typically, a 90 cm length was employed. In both twin and merged jet, matrices were deposited at the rate of 2 mmol/h from each sample manifold onto the cold window. Final spectra were recorded on a Perkin-Elmer Spectrum One Fourier transform infrared spectrometer at 1 cm^{-1} resolution.

Theoretical calculations were carried out on likely intermediates in this study, using the Gaussian 98W suite of programs.[15] Density functional calculations using the hybrid B3LYP functional were used to locate energy minima, determine structures, and calculate vibrational spectra. Final calculations with full geometry optimization employed the 6-311G+(d,2p) and LANL2DZ basis sets, after initial calculations with smaller basis sets were run to approximately locate energy minima.

10.1021/jp020118x CCC: $22.00

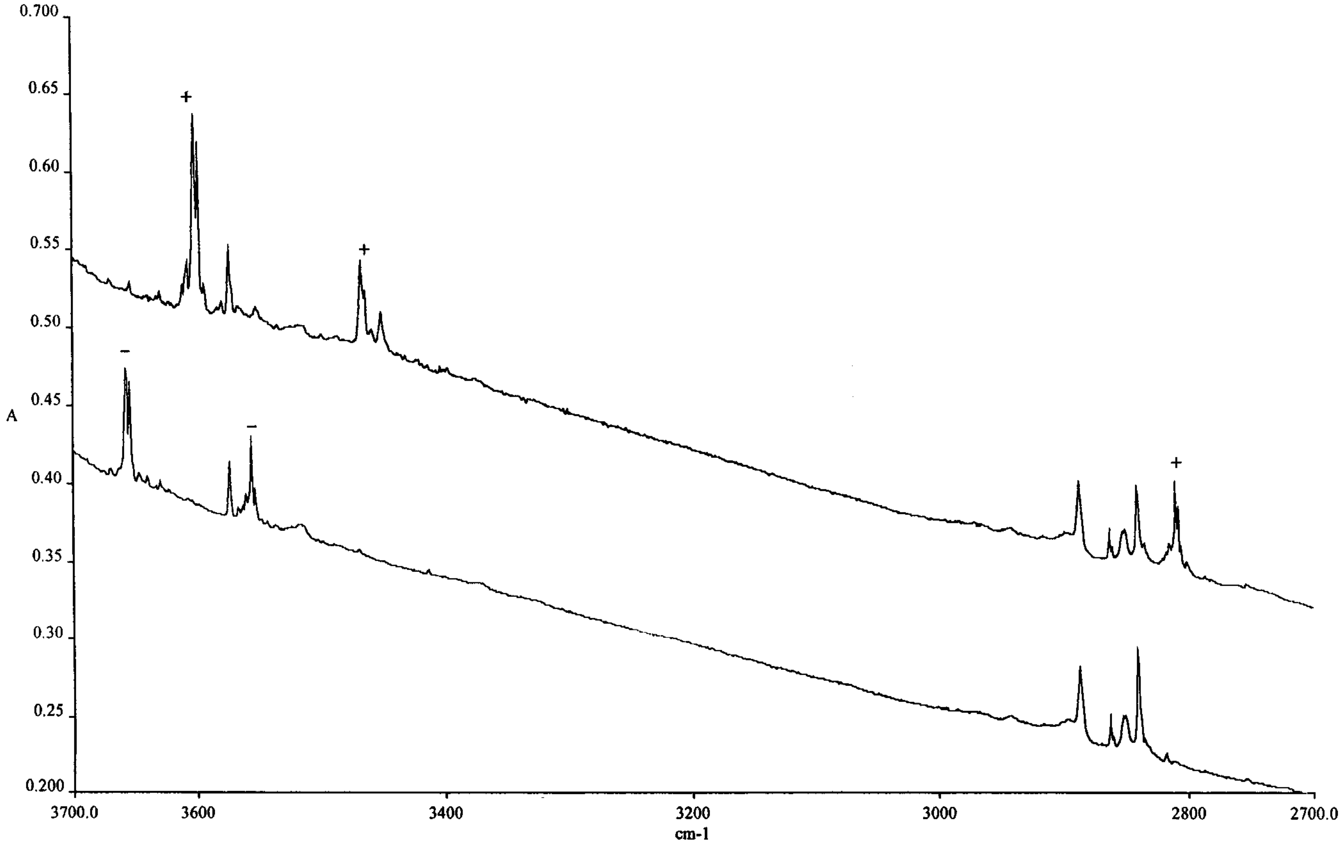

Figure 1. Infrared spectra of a matrix prepared by the twin jet co-deposition of a sample of $Ar/OVCl_3 = 250$ with a dilute sample of Ar/H_2O. The lower trace is before irradiation; the upper trace shows the spectrum after irradiation. Bands marked with a "+" grew as a result of irradiation; bands marked with a "−" were destroyed by irradiation.

Experimental Results

Prior to any co-deposition experiments, blank experiments were run on each of the reagents used in this study.[16−20] In each case, the blanks were in good agreement with literature spectra and with blanks run previously in this laboratory. The actual $^{18}O/^{16}O$ ratio in the $H_2{}^{18}O$ blank, as determined by relative parent band intensities, was approximately 2/1, while in the D_2O experiments the D/H ratio was approximately 1/1 in the initial experiments and increased to as high as 4/1 when additional experiments were conducted. Each blank experiment was then irradiated by the H_2O/Pyrex filtered output of a 200 W Hg arc lamp for 1.5 h. No changes were observed in any of the blank spectra as a result of irradiation. Weak bands due to HCl impurity were noted in all of the $CrCl_2O_2$ and $OVCl_3$ blank experiments.[21]

$OVCl_3 + H_2O$. In an initial twin jet experiment, a sample of $Ar/H_2O = 500$ was co-deposited with a sample of $Ar/OVCl_3 = 250$. After 20 h of deposition, weak product bands were observed at 446, 1534, 3557, and 3650 cm^{-1}, in addition to quite intense absorptions of both parent species. When this sample was annealed to 30 K and an additional spectrum recorded, these four bands were seen to grow slightly. Growth was also seen in parent bands of H_2O dimer, with a slight reduction in the intensity of the H_2O monomer bands. This matrix was then irradiated for 1.5 h with the filtered ($\lambda > 300$ nm) output of a medium-pressure Hg arc lamp. The weak bands noted above all disappeared upon irradiation, and a set of new bands were observed, at 433, 798, 2808, 3450, 3466, and 3598 cm^{-1}. Several of these bands were split into doublets or multiplets. Figure 1 shows spectra of this matrix before and after irradiation.

Numerous additional experiments were conducted, depositing these two reagents into argon matrices at different concentrations, using twin jet deposition. The exact concentration of H_2O in these matrices was difficult to control due to the absorption of H_2O on the walls of the sample manifold and deposition lines. Nonetheless, a range of concentrations of H_2O in argon was explored and the same results were obtained throughout. The weak bands formed upon initial sample deposition were observed reproducibly, were all destroyed by irradiation, and the second set of weak (but somewhat more intense) bands grew in upon irradiation. While the absolute intensities of these bands were low (0.01−0.10 O.D.), the relative intensities of the bands in each set appeared to be consistent over all of the experiments.

A series of twin jet experiments were also conducted in which N_2 was used as the matrix gas. Qualitatively similar results were obtained, with weak bands formed upon initial deposition near 440, 475, 1572, and 3592 cm^{-1}. These were destroyed by irradiation, leading to weak new features at 436, 483, 780, 805, 2750, 2768, 2815, 3437, and 3451 cm^{-1}. These results and band positions were reproducible over the seven experiments in which N_2 was employed.

A set of twin jet experiments was undertaken in which samples of $Ar/OVCl_3$ were co-deposited with samples of $Ar/H_2{}^{18}O$. Inasmuch as the isotopic enrichment was not 100% due to exchange, the bands described above were seen, with lower intensity. In addition, in the better (higher yield) experiments at higher sample concentrations, a new absorption was observed at 3549 cm^{-1}. When this sample was irradiated, the above irradiation products were observed, along with bands at 434, 771, 3436, and 3586 cm^{-1}. These were reproducible over several experiments at higher sample concentrations. In the lower

TABLE 1: Band Positions and Assignments for $Cl_2V(O)OH$ in Argon Matrices

$Cl_2V(O)OH$	$Cl_2V(O)^{18}OH$	$Cl_2V(O)OD$	assignment
433 cm^{-1}	434 cm^{-1}		VCl_2 asym. st.
798	771	779 cm^{-1}	V−O stretch
3450[a]	3436	2562	O−H stretch[b]
3598	3586	2661	O−H stretch[c]

[a] Multiplet. [b] Interacting with cage-paired HCl. [c] Not interacting with cage-paired HCl.

TABLE 2: Band Positions and Assignments for $ClCr(O)_2OH$ in Argon Matrices

$ClCr(O)_2OH$	$ClCr(O)_2{}^{18}OH$	$ClCr(O)_2OD$	assignment
479 cm^{-1}	479 cm^{-1}	477 cm^{-1}	Cr−Cl stretch
755	725	726	Cr−O stretch
3437	3426	2539	O−H stretch

concentration experiments, the bands were so weak that they could not be conclusively identified.

Samples of Ar/$OVCl_3$ were also co-deposited with samples of Ar/D_2O in several experiments. Due to impurity H_2O from other sources and exchange with adsorbed species, the degree of deuteration was less than 100%; in the best experiments, D/H = 4. In a typical experiment involving these two reagents, bands were seen upon deposition and prior to irradiation, at 446, 1145, 1362, and 2718 cm^{-1}. All four bands grew slightly upon sample annealing to 30 K. Irradiation of this sample with $\lambda > 300$ nm completely destroyed these four bands, and led to growth of bands at 560, 779, 798, 2034, 2562, 2661, 3465, and 3598 cm^{-1}. The bands at 798, 3465, and 3598 cm^{-1} matched the above product bands with normal isotopic water. These product bands were reproducible in all of the experiments conducted with this pair of reagents. Table 1 summarizes product bands positions for the photochemical products of $OVCl_3$ with H_2O and its isotopomers in argon matrices.

$CrCl_2O_2 + H_2O$. Similar experiments were conducted in which samples of Ar/$CrCl_2O_2$ = 150 were co-deposited with samples of Ar/ H_2O, Ar/$H_2{}^{18}O$, and Ar/D_2O in twin jet experiments. Very weak bands were observed prior to deposition for each pair of reagents. These bands were destroyed with Hg arc irradiation with $\lambda > 300$ nm, and new product bands observed. For example, when H_2O was employed, product bands were noted after irradiation at 479, 754, 2817, and 3435 cm^{-1}, rather close to product bands reported above for $OVCl_3/H_2O$. Product bands for the photochemical reaction of $CrCl_2O_2$ with water isotopomers are summarized in Table 2, and displayed in Figures 2 and 3. Over several experiments with each pair of reagents, the product bands were weak but reproducible, and appeared to maintain a constant intensity ratio with respect to one another. Finally, the merged jet co-deposition of $CrCl_2O_2$ and H_2O was explored as well; results very similar to those from the twin jet experiments were obtained.

Results of Calculations

Previous studies[7−13] have shown (and will be discussed below) that photochemical elimination of HCl from the initial reactants is a likely mode of reaction, yielding $Cl_2V(O)OH$ and $ClCr(O)_2OH$. Consequently, DFT calculations were undertaken on these two species using the B3LYP hybrid functional and basis sets as high as 6-311G+(d,2p) and LANL2DZ. Both compounds optimized to energy minima on their respective potential energy surfaces, with all positive vibrational frequencies. Table 3 gives the key geometric parameters calculated for each. Vibrational frequencies were also calculated for the normal isotope, the ^{18}O-labeled isotopomer and the ^2H-labeled isotopomer, for comparison to experimental spectra. The results of these calculations are given in Tables 4 and 5. Calculations were also carried out for the double HCl elimination product $ClVO_2$. This species optimized as well to a stable minimum at the B3LYP/6-311G+ level of theory, and vibrational spectra were calculated as well.

Discussion

Weak bands were observed upon initial co-deposition of samples of either Ar/$OVCl_3$ or Ar/$CrCl_2O_2$ with samples of Ar/H_2O; with $OVCl_3$ these bands were located at 446, 1534, 3557, and 3650 cm^{-1}. These bands grew somewhat upon annealing, and were completely destroyed with Hg arc irradiation. These bands were formed under the conditions of shortest reaction time and lowest reaction temperature, namely in the twin jet deposition experiments, where mixing of the two reactants occurs on the surface of the condensing matrix. This indicates the absorbing species is the initial intermediate in the reaction between $OVCl_3$ and H_2O. It is also important to note that each of the four bands lies near a parent mode of one of the reagents; the 446 cm^{-1} band is to the red of the intense 505 cm^{-1} of $OVCl_3$, while the bands at 1534, 3557, and 3650 cm^{-1} lie near the bending and the two stretching modes of H_2O, respectively. Further, the isotopic dependence of each of these bands mirrored the isotopic dependence of the nearby parent mode. These observations are indicative of the formation of a molecular complex between the two reacting species, where each subunit is perturbed in the complex, yet maintains its molecular identity.[22] On this basis, these initial weak product bands are assigned to a molecular complex between either $OVCl_3$ or $CrCl_2O_2$, and H_2O and its isotopomers in argon and nitrogen matrices.

The stoichiometry of the complexes is not as readily determined. However, the observation of only a single product after co-deposition over a wide range of concentrations suggest that the stoichiometry is 1:1. This is particularly true in those experiments where H_2O was only present at impurity levels (3000−5000/1), and since the yield of the complex was very low. Certainly, it would be difficult to envision formation of higher complexes (e.g., 2:1 or 1:2) without also forming the 1:1 complex. The observation of a single product argues against this, and for the formation of the 1:1 complex. Consequently, the bands described above are assigned to the 1:1 molecular complexes $Cl_3VO{\cdot}OH_2$ and $Cl_2CrO_2{\cdot}OH_2$. *These species represent the initial intermediates in the reactions between each pair of reagents.* Band assignments are straightforward, since each band represents the nearby parent band shifted upon formation of the molecular complex. The complex appears to be quite weakly bound, and a number of fundamentals are not shifted sufficiently far away from parent $OVCl_3$ or $CrCl_2O_2$ to be detected in these experiments, since most of the parent molecules are trapped and isolated unreacted.

Photochemical Products

The 1:1 molecular complex is clearly very sensitive to ultraviolet irradiation, as bands due to this complex were destroyed by 1.5 h of irradiation with light of $\lambda > 300$ nm. Similar results were observed for a number of related complexes, including the complexes of NH_3 and CH_3OH with $OVCl_3$ and $CrCl_2O_2$. In each of these cases, it was shown conclusively that complex destruction occurred through HCl elimination, after absorption of a photon. The HCl produced in these systems, however, was trapped within the matrix cage with the second

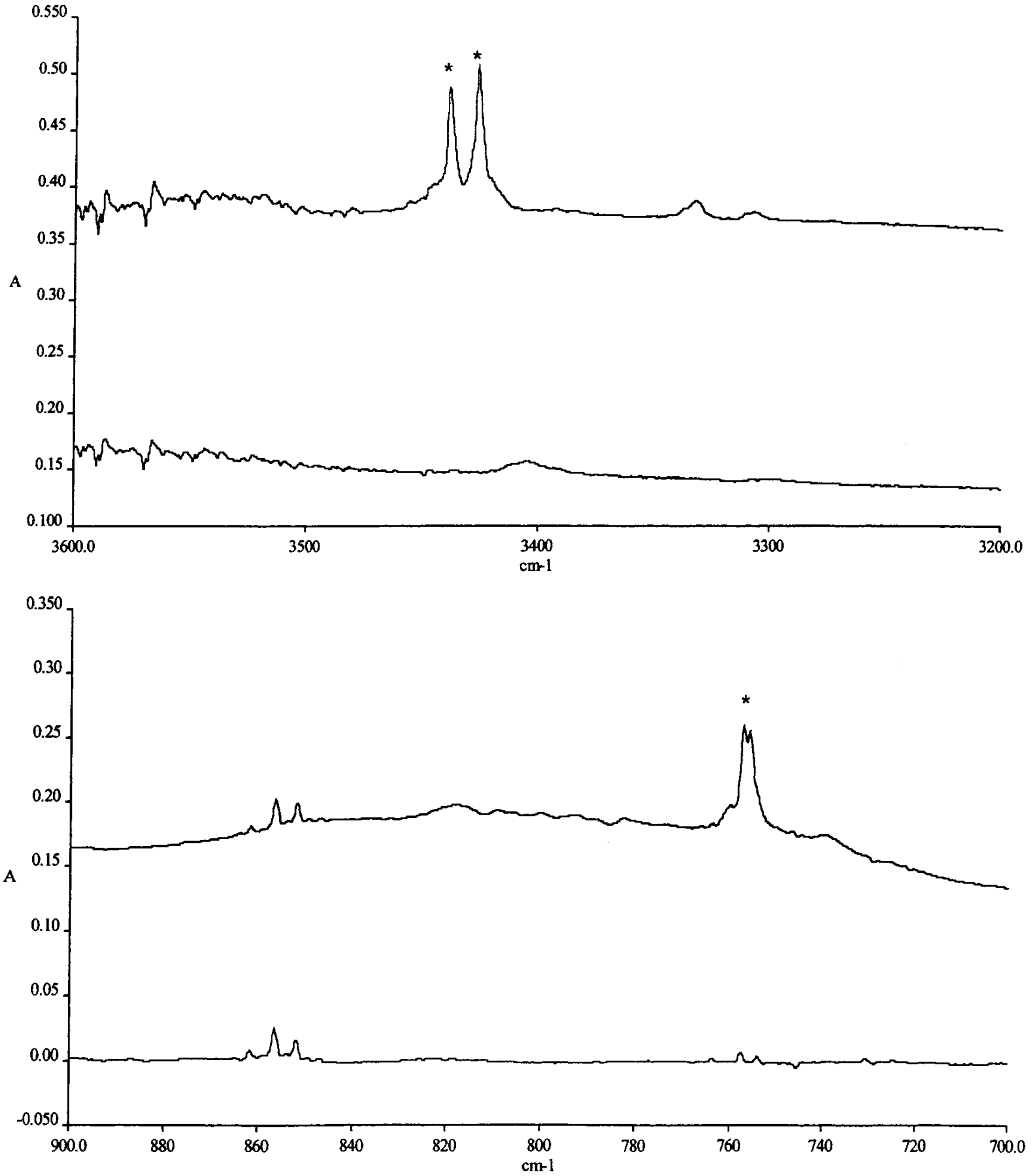

Figure 2. Infrared spectra in selected regions of a matrix prepared by the co-deposition of a sample of $Ar/CrCl_2O_2 = 150$ with a dilute sample of H_2O. The lower trace in each frame is the spectrum before irradiation; the upper spectrum was recorded after irradiation. Bands marked with an * appear upon irradiation.

photoproduct (for example, $Cl_2V(O)NH_2$ in the $OVCl_3/NH_3$ system). The HCl spectrum, then, was that of weakly hydrogen-bonded HCl, with bands appearing between 2750 and 2800 cm^{-1}, shifted from isolated monomeric HCl which absorbs at 2863 and 2888 cm^{-1} in solid argon.[24,25] Similar absorptions were seen in the present experiments, at 2808 cm^{-1} with $OVCl_3$ and 2817 cm^{-1} with $CrCl_2O_2$ in argon matrices). *These bands did not shift upon ^{18}O substitution*, but did shift upon deuteration to 2034 cm^{-1} in the $OVCl_3$ experiments, and to a multiplet centered at 2028 cm^{-1} in the $CrCl_2O_2$ experiments. This is precisely the isotopic dependence anticipated for HCl. In addition, the ν_H/ν_D ratios of $2808/2034 = 1.38$ and $2817/2028 = 1.39$ are almost identical to that observed for both gas-phase[23] and matrix-isolated[24,25] HCl, namely 1.38. Given the isotopic behavior of these bands and the analogy to a number of well-established systems, the bands at 2808 and 2817 cm^{-1} are assigned to photoproduced HCl, arising from the decomposition of the initial 1:1 molecular complexes. Further, the HCl that is produced is trapped within the same matrix cage, and weakly hydrogen bonded to the species responsible for the remainder of the photochemical bands.

The photochemical product for each system is clearly identified with the species resulting from an HCl elimination process from the molecular complex. In the previous studies[7-10] of the $OVCl_3 + CH_3SH$, $CrCl_2O_2 + CH_3OH$, and $OVCl_3 + CH_3OH$ systems, only one HCl elimination product was possible. This was the product arising from the elimination of one HCl unit from the complex, yielding $Cl_2V(O)SCH_3$, $ClCr(O)_2OCH_3$, and $Cl_2V(O)OCH_3$, respectively. In the previous studies[11,12] of the $OVCl_3 + NH_3$ and $CrCl_2O_2$ systems, elimination of either one or more HCl molecules was possible. These studies demonstrated that only a single elimination of HCl occurs. In the present study the possibility of the elimination of either one or two HCl units from the molecular complex is

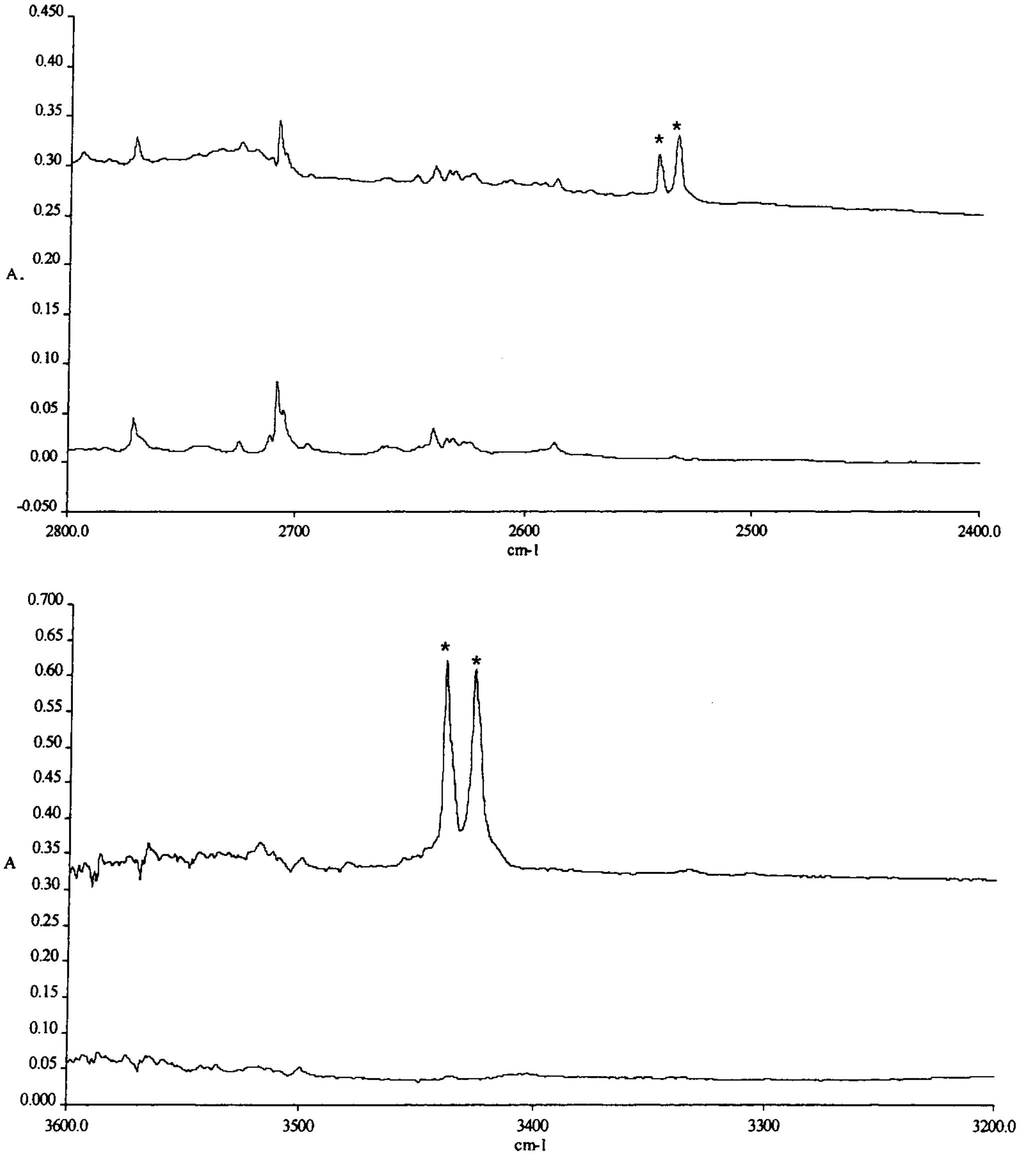

Figure 3. Infrared spectra in the O−H and O−D stretching regions of a matrix prepared by the co-deposition of a sample of Ar/$CrCl_2O_2$ = 150 with a dilute sample of Ar/D_2O (with significant H_2O impurity). The lower trace in each frame is the spectrum before irradiation; the upper spectrum was recorded after irradiation. Bands marked with an * appear upon irradiation.

TABLE 3: Key Computed Structural Parameters[a]

parameter	$Cl_2V(O)OH$	$ClCr(O)_2OH$
$R_{M=O}$	1.56 Å	1.55 Å
R_{M-Cl}	2.16 Å	2.14 Å
R_{M-O}	1.75 Å	1.75 Å
R_{O-H}	0.96 Å	0.97 Å
α_{M-O-H}	124.6°	117.1°
$\alpha_{O=M-O}$	108.7°	109.0°
α_{Cl-M-O}	110.1°	109.7°
spin multiplicity	1	1

[a] Computed at the B3LYP/6-311G+(d,2p) level of theory.

present, to yield either $ClCr(O)_2OH$ or CrO_3 from $CrCl_2O_2$·OH_2, and either $Cl_2V(O)OH$ or $ClVO_2$ from Cl_3VO·OH_2.

Distinguishing between these possibilities is straightforward. First, a product band was observed for each system above 3400 cm^{-1}, a region attributable primarily to O−H stretching modes. Of course, only one possible product for each system contains an O−H bond. In addition, *all of the product bands for each system shifted with deuterium substitution*, indicating that the absorbing species must contain at least one D atom. This eliminates CrO_3 and $ClVO_2$ as possible product species, and thus requires a single HCl elimination from each complex, to form $Cl_2V(O)OH$ and $ClCr(O)_2OH$, respectively, from Cl_3VO·OH_2 and $CrCl_2O_2$·OH_2. This conclusion is strongly supported by the quite good fit between the experimental spectrum of each photochemical product, and the infrared spectra and isotopic shifts calculated by DFT methods, as discussed below. Thus, the photochemical products for these two systems are identified as $Cl_2V(O)OH$ and $ClCr(O)_2OH$. One complicating factor in this identification is the observation of two O−H stretching modes in the $OVCl_3$/H_2O studies, one at 3598 cm^{-1} and the other a doublet centered at 3458 cm^{-1} (see Figure 1). The higher energy band is more characteristic of a free O−H oscillator (and is in much better agreement with the calculated O−H stretching band position for $Cl_2V(O)OH$), while the lower energy band is more characteristic of a weakly perturbed O−H oscillator. Since HCl is formed as a photoproduct in these experiment, it is trapped in the same matrix cage with the $Cl_2V(O)OH$ species. It is likely that the 3458 cm^{-1} absorption is due to a configuration in the matrix cage where the O−H moiety is interacting with the trapped HCl, while the 3598 cm^{-1} band is due to a configuration where they are trapped in a geometry that does

TABLE 4: Calculated (B3LYP 6-311G+(d,2p)) and Observed Frequencies and Isotopic Shifts for Cl2V(O)OH

normal isotope				^{18}O		^{2}H		
calcd freq.[a]	calcd I_{rel}	expt. freq.	expt. I_{rel}	calcd shift	ex. shift	calcd shift	ex. shift	description
415 (403)	0.03			−2		−1		VCl_2 st.
431 (418)	0.17	433	0.2	−4	1	−93		VCl_2 st.
523 (507)	0.84			−2		−14		V−O−H bend
650 (631)	0.56			−10		−129		V−O−H bend
794 (770)	0.44	798	0.45	−26	−27	−21	−19	V−O stretch
1118 (1084)	0.63			0		0		V=O stretch
3842 (3727)	1	3598	1	−12	−12	−1044	−937	O−H stretch

[a] Unscaled frequencies (scaled frequencies, with a 0.97 scale factor, are given parenthetically).

TABLE 5: Calculated (B3LYP 6-311G+(d,2p)) and Observed Frequencies and Isotopic Shifts for ClCr(O)2OH

normal isotope					^{18}O			^{2}H			
calcd freq.[a] B3LYP	calcd I_{rel}	calcd freq.[a] LANL2DZ	expt. freq.	expt. I_{rel}	calcd shift B3LYP	calcd shift LANL2DZ	ex. shift	calcd shift B3LYP	calcd shift LANL2DZ	ex. shift	description
486	0.43	455	479	0.18	0	−1	0	−2	−12	−2	Cr−Cl stretch
741	0.89	586			−23	−9			−114		Cr−O−H bend
774	0.14	816	755	0.64	−12	−27	−30	17	−25	−29	Cr−O stretch
1089	0.8	1074			0	−1			0		Cr=O stretch
1103	0.84	1097			0	0			0		Cr=O stretch
3810	1	3726	3437	1	−13	−13	−11	−1037	−998	−898	O−H stretch

[a] Unscaled frequencies.

not allows interaction. The former configuration would then be responsible for the shifted H−Cl stretching bands near 2800 cm^{-1} while the latter should give rise to absorption near 2880 cm^{-1}. Weak bands of unperturbed HCl are seen near 2880 cm^{-1} in all experiments, as it is very difficult to remove traces of residual HCl from $OVCl_3$ and $CrCl_2O_2$. In the former configuration, where the two species are interacting within the matrix cage, both the O−H and the H−Cl stretching modes are perturbed and red-shifted. This suggests that both are acting as proton donors as well as proton acceptors, in a cyclic structure.

The theoretical calculations also provide calculated spectra and isotopic shifts for comparison to experiments. Tables 4 and 5 compare the calculated infrared band positions, intensities, and isotopic shifts for $Cl_2V(O)OH$ and $ClCr(O)_2OH$ to the experimental band positions. For $Cl_2V(O)OH$, the calculations predict 7 bands above 400 cm^{-1}, the spectral limit of the spectrometer. One of these is very close to the instrumental limit, while a second is very close to the parent V=O stretch, is strongly overlapped by the intense parent band, and thus not observed. The V−O−H bending modes are predicted to be moderately intense. One should come very near an intense mode of parent $OVCl_3$ and is obscured, while the second is not observed. It is not clear why, other than calculated intensities are known to be quite approximate. The remaining three modes, the O−H stretch, the V−O stretch, and the V−Cl stretch are all observed, and there is relatively good agreement between experiment and theory, as shown in Table 4. For $CrCl_2O_2$, the B3LYP/6-311G+(d,2p) calculations have the Cr−O−H bend and the Cr−O stretch very close in energy, and substantially mixed in character. The mixing is greatly reduced for the ^{2}H isotopomer, since the bending mode shifts strongly to lower energy. As a result of this mixing, the isotopic shifts and intensities are not well reproduced by the calculations. However, calculations at the B3LYP/LANL2DZ level of theory show much greater separation of these two modes, with very little mode mixing, and the experimental isotopic shifts are reproduced quite well. In both cases, the Cr−Cl and O−H stretches are modeled well, as shown in Table 5. Overall, the theoretical calculations support the experimental identification of these two new species.

Further Considerations

The conclusions reached here suggest that the first step in reaction between either $CrCl_2O_2$ or $OVCl_3$ and H_2O is the formation of a 1:1 molecular complex, which undergoes HCl elimination in a second step, to form the observed intermediates. This mechanism is consistent with the previous studies of the reaction chemistry of $CrCl_2O_2$ and $OVCl_3$. Overall, however, the product yield in the present study was much less than that in the previous studies. Given this mechanism, the yields of $ClCr(O)_2OH$ and $Cl_2V(O)OH$ are limited by the amount of 1:1 complex formed during the deposition process. While $OVCl_3$ and $CrCl_2O_2$ are strong Lewis acids, H_2O is the weakest of the bases employed as a reaction partner for these compounds.[26] The low basicity of H_2O very likely limits the amount of complex formed during matrix condensation, and hence the yields of $ClCr(O)_2OH$ and $Cl_2V(O)OH$ thereafter. In as much as the yield of product was not increased during merged jet deposition, it is not clear whether the thermal, gas-phase reaction proceeds via this mechanism. Certainly, there is no evidence that it does not. Further study of this question is needed.

Acknowledgment. The authors gratefully acknowledge support of this research by the National Science Foundation through Grant CHE 9877076. B.L.S. acknowledges the Women in Science and Engineering Program at the University of Cincinnati for a summer fellowship. A. Gudmundsdottir is gratefully acknowledged for computer time.

References and Notes

(1) Crans, D. C.; Chen, H.; Felty, R. A. *J. Am. Chem. Soc.* **1992**, *114*, 4543.

(2) Yajima, A.; Matsuzaki, R.; Saeki, Y. *Bull. Chem. Soc. Jpn.* **1978**, *51*, 1098.

(3) Field, M. N.; Parkin, I. P. *J. Mater. Chem.* **2000**, *10*, 1863.

(4) Craddock, S.; Hinchliffe, A. *Matrix Isolation*; Cambridge University Press: Cambridge, 1975.

(5) Hallam, H. E. *Vibrational Spectroscopy of Trapped Species*; John Wiley: New York, 1973.

(6) *Chemistry and Physics of Matrix Isolated Species*; Andrews, L., Moskovitz, M., Eds.; Elsevier Science Publishers: Amsterdam, 1989.

(7) Ault, B. S. *J. Am. Chem. Soc.* **1998**, *120*, 6105.

(8) Ault, B. S. *J. Mol. Struct*. **2000**, *526*, 227.

(9) Ault, B. S. *J. Phys. Chem. A* **1999**, *103*, 11474.

(10) Ault, B. S. *J. Phys. Chem. A* **2000**, *104*, 11796.

(11) Ault, B. S. *J. Phys. Chem. A* **2001**, *105*, 4758.

(12) Anderson, S. R.; Ault, B. S. *J. Phys. Chem. A* **2002**, *106*, 1419.

(13) Ault, B. S. *J. Am. Chem. Soc*. **1978**, *100*, 2426.

(14) Carpenter, J. D.; Ault, B. S. *J. Phys. Chem.* **1991**, *95*, 3502.

(15) Frisch, M. J.; Trucks, G. W.; Schlegel, H. B.; Scuseria, G. E.; Robb, M. A.; Cheeseman, J. R.; Zakrzewski, V. G.; Montgomery, J. A., Jr.; Stratmann, R. E.; Burant, J. C.; Dapprich, S.; Millam, J. M.; Daniels, A. D.; Kudin, K. N.; Strain, M. C.; Farkas, O.; Tomasi, J.; Barone, V.; Cossi, M.; Cammi, R.; Mennucci, B.; Pomelli, C.; Adamo, C.; Clifford, S.; Ochterski, J.; Petersson, G. A.; Ayala, P. Y.; Cui, Q.; Morokuma, K.; Malick, D. K.; Rabuck, A. D.; Raghavachari, K.; Foresman, J. B.; Cioslowski, J.; Ortiz, J. V.; Baboul, A. G.; Stefanov, B. B.; Liu, G.; Liashenko, A.; Piskorz, P.; Komaromi, I.; Gomperts, R.; Martin, R. L.; Fox, D. J.; Keith, T.; Al-Laham, M. A.; Peng, C. Y.; Nanayakkara, A.; Challacombe, M.; Gill, P. M. W.; Johnson, B.; Chen, W.; Wong, M. W.; Andres, J. L.; Gonzalez, C.; Head-Gordon, M.; Replogle, E. S.; Pople, J. A. *Gaussian 98, Revision A.9*; Gaussian, Inc.: Pittsburgh, PA, 1998.

(16) Varetti, E. L.; Muller, A. *Spectrochim. Acta* **1978**, *34A*, 895.

(17) Filgueira, R. R.; Fournier, L. L.; Varetti, E. L. *Spectrochim. Acta* **1982**, *38A*, 965.

(18) Ayers, G. P.; Pullin, A. D. E. *Spectrochim. Acta* **1976**, *32A*, 1629.

(19) Tursi, A. J.; Nixon, E. R. *J. Chem. Phys*. **1970**, *52*, 1521.

(20) Ayers, G. P.; Pullin, A. D. E. *Spectrochim. Acta* **1976**, *32A*, 1689.

(21) Ault, B. S. *J. Mol. Struct.* **2000**, *526*, 97.

(22) Ault, B. S. *Rev. Chem. Intermed.* **1988**, *9*, 233.

(23) Nakamoto, K. *Infrared and Raman Spectra of Inorganic and Coordination Compounds*, 5th ed.; Wiley-Interscience: New York, 1997.

(24) Barnes, A. J.; Hallam, H. E.; Scrimshaw, G. F. *Trans. Faraday Soc*. **1969**, *65*, 3150.

(25) Maillard, D.; Schriver, A.; Perchard, J. P. *J. Chem. Phys*. **1979**, *71*, 505.

(26) Lias, S. G.; Liebman, J. F.; Levin, R. D. *J. Phys. Chem. Ref. Data* **1984**, *13*, 695.